Genetic Inactivation of ERK1 and ERK2 in Chondrocytes Promotes Bone Growth and Enlarges the Spinal Canal

Arjun Sebastian,[1] Takehiko Matsushita,[1] Aya Kawanami,[1] Susan Mackem,[2] Gary E. Landreth,[3] Shunichi Murakami[1,4]

[1]Department of Orthopaedics, Case Western Reserve University, 10900 Euclid Avenue, Cleveland, Ohio 44106, [2]Cancer and Developmental Biology Laboratory, National Cancer Institute, Frederick, Maryland, [3]Department of Nuerosciences, Case Western Reserve University, Cleveland, Ohio, [4]Department of Genetics, Case Western Reserve University, Cleveland, Ohio

ABSTRACT: Activating mutations in FGFR3 cause the most common forms of human dwarfism: achondroplasia and thanatophoric dysplasia. In mouse models of achondroplasia, recent studies have implicated the ERK MAPK pathway, a pathway activated by FGFR3, in creating reduced bone growth. Our recent studies have indicated that increased Fgfr3 and ERK MAPK signaling in chondrocytes also causes premature synchondrosis closure in the cranial base and vertebrae, accounting for the sometimes fatal stenosis of the foramen magnum and spinal canal in achondroplasia. Conversely, whether the decrease—or inactivation—of ERK1 and ERK2 promotes bone growth and delays synchondrosis closure remains to be investigated. In this study, we inactivated ERK2 in the chondrocytes of ERK1-null mice using the Col2a1-Cre and Col2a1-CreER transgenes. We found that the genetic inactivation of ERK1 and ERK2 in chondrocytes enhances the growth of cartilaginous skeletal elements. We also found that the postnatal inactivation of ERK1 and ERK2 in chondrocytes delays synchondrosis closure and enlarges the spinal canal. These observations make ERK1 and ERK2 an attractive target for the treatment of achondroplasia and other FGFR3-related skeletal syndromes. © 2010 Orthopaedic Research Society. Published by Wiley Periodicals, Inc. J Orthop Res

Keywords: ERK; chondrocytes; bone growth; synchondrosis; achondroplasia

The extracellular signal-regulated kinase (ERK) mitogen-activated protein kinase (MAPK) pathway consists of a series of kinases that play important roles in skeletal development. The ERK MAPK pathway is activated by various cytokines and growth factors, including family members of fibroblast growth factor (FGF). Activating mutations in FGF receptor 3 (FGFR3) cause the most common forms of human dwarfism—achondroplasia, thanatophoric dysplasia, and hypochondroplasia.[1–6] Mutations in the signaling molecules in the ERK MAPK pathway also cause a number of human skeletal disorders, including Noonan, Costello, and cardio-facio-cutaneous syndromes.[7–9]

The growth inhibitory roles of FGFR3 have been demonstrated in a number of mouse models and human skeletal syndromes. Mice that express a gain-of-function mutant of Fgfr3 show a dwarf phenotype similar to the human dwarfisms achondroplasia and thanatophoric dysplasia.[10–13] In contrast, Fgfr3-null mice show skeletal overgrowth similar to that seen in human camptodactyly, tall stature, and hearing loss (CATSHL) syndrome, which is caused by a loss-of-function mutation in FGFR3.[14–16] Several lines of evidence have indicated that the ERK MAPK pathway is a critical downstream effector of Fgfr3. Growth plate chondrocytes expressing a human achondroplasia mutant of Fgfr3, for example, show increased levels of phosphorylated ERK1 and ERK2 and their upstream kinase MEK1.[17,18] Furthermore, mice expressing a constitutively active mutant of MEK1 in chondrocytes show an achondroplasia-like dwarfism.[17] In addition, the overexpression of C-type natriuretic peptide (CNP) in chondrocytes causes

skeletal overgrowth and rescues the dwarf phenotype in a mouse model of achondroplasia.[18] One of the actions of CNP is to inhibit the ERK MAPK pathway.[18,19]

Recent work in our laboratory has indicated that Fgfr3 and the ERK MAPK pathway also regulate synchondrosis closure.[20] A synchondrosis consists of two opposed growth plates with a common zone of resting chondrocytes. We found premature synchondrosis closure in the vertebrae and the cranial base of human samples of homozygous achondroplasia and thanatophoric dysplasia. We also observed premature synchondrosis closure in the cranial base and vertebrae of mice expressing the Fgfr3 G374R achondroplasia mutant and mice expressing a constitutively active MEK1 mutant in chondrocytes. These observations strongly suggest that premature synchondrosis closure accounts for the foramen magnum and spinal canal stenosis in achondroplasia. A common and serious complication of achondroplasia,[6,21] foramen magnum and cervical spinal stenosis associated with compression of the brainstem and spinal cord can lead to sudden death during early childhood.[22] In addition, spinal canal stenosis can cause other neurologic complications such as radiculopathy, claudication, and paraparesis.

While increased ERK MAPK signaling has been implicated in reduced bone growth and premature synchondrosis closure, whether or not the specific inactivation of ERK1 and ERK2 in chondrocytes indeed accelerates bone growth and delays synchondrosis closure has remained to be investigated. In this study, we examined the effects of the genetic inactivation of ERK1 and ERK2 on bone growth and synchondrosis closure. We show here that the prenatal inactivation of ERK1 and ERK2 in chondrocytes results in increased growth of the long bones and vertebral bodies. We further show that the postnatal inactivation of ERK1 and ERK2 in chondrocytes delays synchondrosis closure in the

Correspondence to: Shunichi Murakami (T: 216-368-1371; F: 216-368-1332; E-mail: shun@case.edu)

vertebrae and enlarges the spinal canal. These observations clearly demonstrate the potential of targeting ERK1 and ERK2 for promoting bone growth and preventing premature synchondrosis closure in human dwarfisms such as achondroplasia.

MATERIALS AND METHODS

Mice

The institutional animal care and use committee approved all animal procedures. *ERK1*-null mice, mice with the floxed *ERK2* allele, and *Col2a1-Cre* transgenic mice were described previously.[23–25] The generation of *ERK1*$^{-/-}$; *ERK2*$^{flox/flox}$; *Col2a1-Cre* (ERK1/2/Col2a1Cre) mice and their initial characterization were reported elsewhere.[26] For postnatal analysis, we used the *Col2a1-CreER* transgene to circumvent the perinatal lethality of ERK1/2/Col2a1Cre mice.[27] One milligram tamoxifen was injected subcutaneously into *ERK1*$^{-/-}$; *ERK2*$^{flox/flox}$; *Col2a1-CreER* (ERK1/2/Col2a1CreER) and control *ERK1*$^{-/-}$; *ERK2*$^{flox/flox}$ mice at postnatal days 4 and 6 (P4, P6), and the animals were sacrificed at P8. Alternatively, 1 mg tamoxifen was injected subcutaneously at P7 and P9, and animals were sacrificed at P14.

Skeletal Preparations and Histological Examination

Skeletal preparations were stained with alcian blue and alizarin red following the standard protocol. Isolated bones were laid next to a ruler and photographed using a dissection microscope, a digital camera, and Leica Application software. Scion Image software (Scion Corporation, Frederick, MD) was used to measure bone lengths. For histological analysis, tissues were fixed in 10% formalin, demineralized in 0.5 M EDTA, and embedded in paraffin. Seven-micrometer thick sections were stained with hematoxylin, eosin, and alcian blue. Photographs were taken using Leica Application software, and the dimensions of the vertebral body and foramen were measured using Scion Image software. For consistency, only the 1st and 2nd lumbar vertebrae were used for the measurement. For immunostaining of CD31, sections were incubated with anti-CD31 (Abbiotec, San Diego, CA) antibody followed by horseradish-peroxidase/Fab polymer conjugate secondary antibody (Invitrogen, Carlsbad, CA, Picture Kit). Non-immune rabbit IgG was used as a control. Color was developed using 3,3′-diaminobenzidine (DAB). Osteoclasts were identified by TRAP staining.[26] TUNEL assay was performed using ApopTag Plus Fluorerscein *In Situ* Apoptosis Detection Kit (Millipore, Ballerica, MA).

Real-Time PCR

Epiphyseal cartilage of the tibia was dissected out from ERK1/2/Col2a1CreER mice and control mice at P8 and stored in RNA*later* (Applied Biosystems, Carlsbad, CA). Tissues were homogenized using Powergen 500 (Fisher, Waltham, MA). RNA was extracted using RNeasy Mini Kit (Qiagen, Germantown, MD) and reverse transcribed by High-Capacity cDNA Reverse Transcription kit (Applied Biosystems). Real-time PCR was performed on the Applied Biosystems 7500 real-time PCR detection system using TaqMan probe sets (Erk2; Mm00442479_m1, Gapdh; 4352932E, Applied Biosystems). The comparative cycle threshold (Ct) method was used to compare gene expression levels.

Statistical Analysis of Data

Statistical analysis was performed using Analyse-it (Analyse-it Software, Leeds, UK). A one-way ANOVA analysis with a post hoc pairwise Scheffe test was used to compare three genotypes at E18.5. The Mann–Whitney test was used to compare ERK1/2/Col2a1CreER and control mice at P8 and P14.

RESULTS

ERK1 and ERK2 Inactivation Enhances the Bone Growth of Proximal Long Bones

The length of each long bone was measured using skeletal preparations of E18.5 embryos (Fig. 1A). While the radius, ulna, and tibia did not show statistically significant differences among genotypes, the humerus and femur were significantly longer in ERK1/2/Col2a1-Cre embryos in comparison to the embryos in which only one allele (*ERK1*$^{-/+}$; *ERK2*$^{flox/flox}$) or three alleles (*ERK1*$^{-/+}$; *ERK2*$^{flox/flox}$; *Col2a1-Cre*) of ERK1/2 were inactivated (Fig. 1B,C). The width of each epiphysis was also measured at its widest point. ERK1/2/Col2a1Cre embryos had significantly wider epiphyses in the proximal and distal humerus and femur (Fig. 1D). ERK1/2/Col2a1Cre embryos also showed wider epiphyses in the distal tibia (data not shown). These observations indicate that the inactivation of *ERK1* and *ERK2* in chondrocytes causes increased bone growth that is more pronounced in the proximal long bones.

ERK1 and ERK2 Inactivation Promotes the Growth of Cartilaginous Vertebrae

We also examined the dimensions of the vertebrae using histological sections of the lumbar vertebrae at E18.5 (Fig. 2A). Hematoxylin, eosin, and alcian blue staining showed a delay in ossification in ERK1/2/Col2a1Cre embryos compared with littermate control embryos (Fig. 2B). While the vertebral body of control embryos was mostly ossified, the vertebral body of ERK1/2/
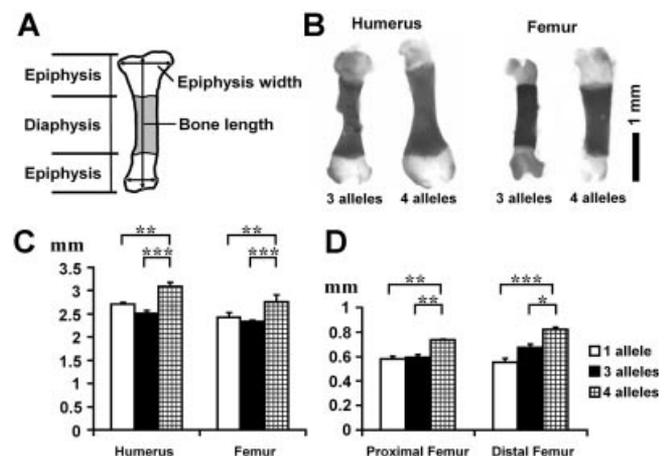

Figure 1. Skeletal preparation and long bone measurements at E18.5. The inactivation of all four alleles of *ERK1* and *ERK2* in chondrocytes promotes bone growth. (A) Scheme of long bone measurement. (B) Skeletal preparation of the femur and humerus of *ERK1*$^{-/+}$; *ERK2*$^{flox/flox}$; *Col2a1-Cre* (three alleles) and *ERK1*$^{-/-}$; *ERK2*$^{flox/flox}$; *Col2a1-Cre* (four alleles) embryos at E18.5. (C) Length of humerus and femur at E18.5. (D) Epiphysis width of proximal and distal femur at E18.5. Values are the mean ± SD. One allele: *ERK1*$^{-/+}$; *ERK2*$^{flox/flox}$ ($n = 10$), three alleles: *ERK1*$^{-/+}$; *ERK2*$^{flox/flox}$; *Col2a1-Cre* ($n = 10$), four alleles: *ERK1*$^{-/-}$; *ERK2*$^{flox/flox}$; *Col2a1-Cre* ($n = 5$). *$p < 0.05$, **$p < 0.01$, ***$p < 0.001$.
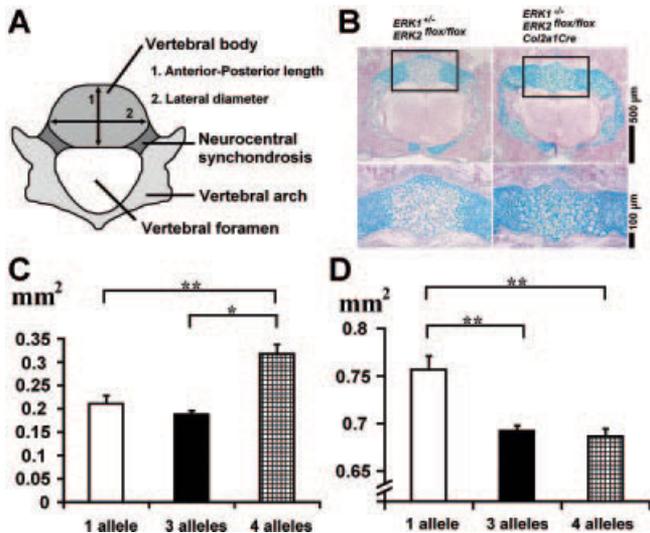
Figure 2. Histology and measurement of lumbar vertebrae at E18.5. (A) Scheme of vertebral measurement. (B) Cross-section of lumbar vertebrae stained with hematoxylin, eosin, and alcian blue showing a delay in the ossification of vertebral body and arch in $ERK1^{-/-}$; $ERK2^{flox/flox}$; *Col2a1-Cre* embryos. The vertebral body (boxed area in the upper panel) is magnified in the lower panel. (C) Cross-sectional area of vertebral body at E18.5. (D) Cross-sectional area of vertebral foramen at E18.5. Values are the mean ± SD. One allele: $ERK1^{-/+}$; $ERK2^{flox/flox}$ ($n = 10$), three alleles: $ERK1^{-/+}$; $ERK2^{flox/flox}$; *Col2a1-Cre* ($n = 10$), four alleles: $ERK1^{-/-}$; $ERK2^{flox/flox}$; *Col2a1-Cre* ($n = 5$). *$p < 0.05$, **$p < 0.01$, ***$p < 0.001$.

Col2a1Cre embryos remained entirely cartilaginous. ERK1/2/Col2a1Cre embryos also showed the persistent presence of hypertrophic chondrocytes both in the vertebral body and arch. The cross-sectional area of the vertebral body was significantly larger in ERK1/2/Col2a1Cre embryos compared with control embryos, indicating increased growth (Fig. 2C). The vertebral body of ERK1/2/Col2a1Cre embryos was larger both in the anterior–posterior and lateral directions (data not shown). In contrast to the measurements of the vertebral body, the cross-sectional area of the vertebral foramen was significantly smaller in ERK1/2/Col2a1Cre embryos compared with control $ERK1^{-/+}$; $ERK2^{flox/flox}$ embryos (Fig. 2D).

Postnatal ERK1 and ERK2 Inactivation Delays Synchondrosis Closure and Enlarges the Spinal Canal

To examine the roles of ERK1/2 in postnatal skeletal development, we inactivated *ERK2* using the *Col2a1-CreER* transgene. Following tamoxifen injection at P4 and P6, *ERK2* expression in the tibial epiphysis was inhibited about 60% in ERK1/2/Col2a1CreER mice at P8 (Fig. 3A). Histological analysis indicated that the overall architecture of the epiphysis was not significantly affected (Fig. 3B). However, ERK1/2/Col2a1CreER mice consistently showed a delay in vascular invasion in the developing secondary ossification centers at P8 (Fig. 3B). We further examined VEGF expression in the epiphyses by real time PCR, but we did not observe differences between ERK1/2/Col2a1CreER and control mice (data not shown). There were no obvious differ-
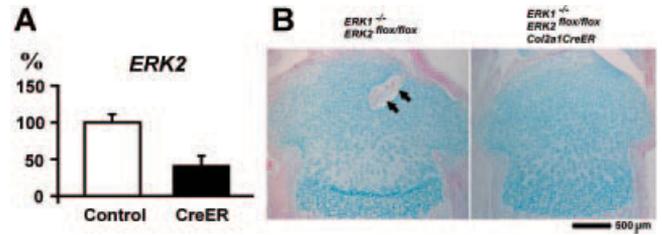

Figure 3. *ERK2* expression and histology of tibial epiphysis of $ERK1^{-/-}$; $ERK2^{flox/flox}$ and $ERK1^{-/-}$; $ERK2^{flox/flox}$; *Col2a1-CreER* mice at P8 following tamoxifen injection at P4 and P6. (A) Real-time PCR analysis of *ERK2* expression in the tibial epiphysis. Control: $ERK1^{-/-}$; $ERK2^{flox/flox}$ ($n = 5$), CreER: $ERK1^{-/-}$; $ERK2^{flox/flox}$; *Col2a1-CreER* ($n = 6$). Values are the mean ± SD. (B) Hematoxylin, eosin, and alcian blue staining of the proximal tibia at P8. Arrows indicate vascular invasion in the developing secondary ossification center.

ences in the dimensions of long bones at P8 and P14 (data not shown).

Histological analysis at P8 and P14 of the vertebrae of ERK1/2/Col2a1CreER mice showed a significant delay in the closure of neurocentral synchondroses, which connect the ossification centers in the vertebral body and arch (Fig. 4A,B). The cross-sectional area of the neurocentral synchondrosis was significantly greater in ERK1/2/Col2a1CreER mice at P8, indicating a delay in cartilage resorption ($p < 0.001$) (Fig. 5A). At P14, the neurocentral synchondroses were closed in five out of eight control $ERK1^{-/-}$; $ERK2^{flox/flox}$ mice, while the synchondroses were open in all seven ERK1/2/Col2a1CreER mice. Furthermore, the cross-sectional area of the vertebral foramen was significantly greater in ERK1/2/Col2a1CreER mice both at P8 ($p < 0.01$) and P14 ($p < 0.01$), indicating that postnatal ERK1/2 inactivation in chondrocytes enlarges the spinal canal (Fig. 5B and data not shown).

Since ERK1/2/Col2a1-CreER mice showed a delay in cartilage resorption, we examined the number of osteoclasts by TRAP staining and examined chondrocyte apoptosis by TUNEL assay. We did not observe obvious differences in the number of osteoclasts and in chondrocyte apoptosis between genotypes (data not shown). We also examined vascular invasion by
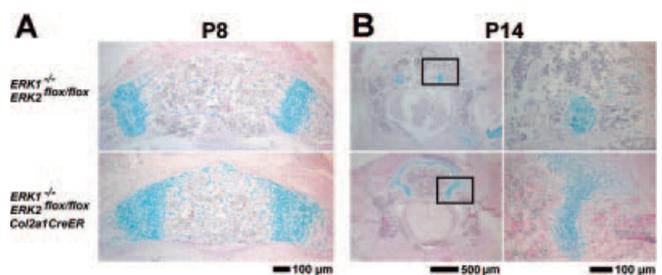

Figure 4. Hematoxylin, eosin, and alcian blue staining of the lumbar vertebrae, showing a delay in synchondrosis closure in $ERK1^{-/-}$; $ERK2^{flox/flox}$; *Col2a1-CreER* mice (lower panels) compared with $ERK1^{-/-}$; $ERK2^{flox/flox}$ mice (upper panels). (A) Vertebral body and neurocentral synchondroses at P8 following tamoxifen injection at P4 and P6. (B) Lumbar vertebrae at P14 following tamoxifen injection at P7 and P9. Neurocentral synchondroses (boxed areas in the left panels) are magnified in the right panels.
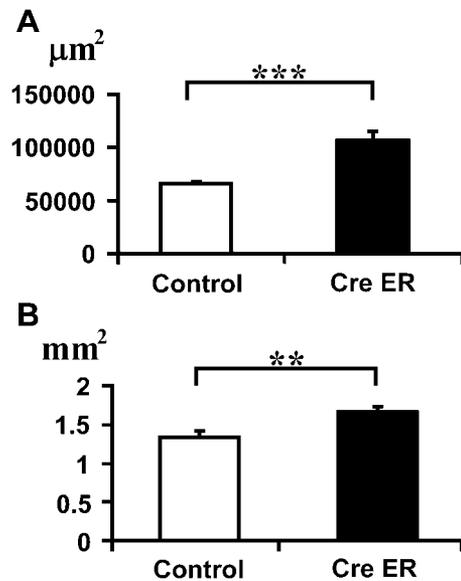
Figure 5. Cross-sectional area of neurocentral synchrosis (A) and vertebral foramen (B) of lumbar vertebrae at P8. Values are the mean ± SD. Control: $ERK1^{-/-}$; $ERK2^{flox/flox}$ ($n = 5$), CreER: $ERK1^{-/-}$; $ERK2^{flox/flox}$; $Col2a1$-CreER ($n = 7$). $**p < 0.01$, $***p < 0.001$.

immunohistochemistry for endothelial marker CD31. We observed decreased staining for CD31 in endothelial cells surrounding the neurocentral synchroses of ERK1/2/Col2a1-CreER mice, suggesting reduced vascular invasion (Fig. 6). This is consistent with the delayed vascularization of the developing secondary ossification center in the long bones. Reduced vascular invasion may at least in part account for the delayed closure of neurocentral synchroses.

DISCUSSION

Our histological analyses and skeletal measurements of ERK1/2/Col2a1Cre embryos clearly indicated that ERK1/2 is a negative regulator of endochondral bone growth. The inactivation of all four alleles of *ERK1* and
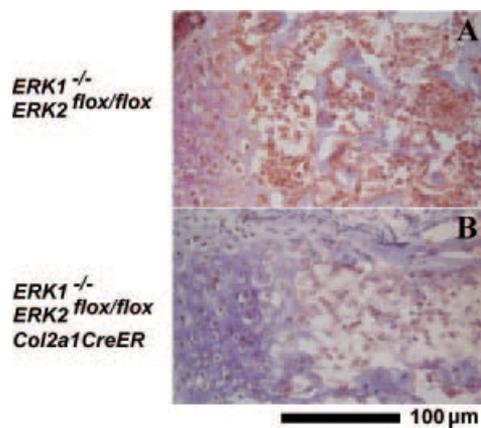

Figure 6. Reduced immunostaining for PECAM-1/CD31 adjacent to the neurocentral synchrosis of $ERK1^{-/-}$; $ERK2^{flox/flox}$; $Col2a1$-$CreER$ mice at P8. (A) $ERK1^{-/-}$; $ERK2^{flox/flox}$, (B) $ERK1^{-/-}$; $ERK2^{flox/flox}$; $Col2a1$-$CreER$.

ERK2 resulted in longer and wider epiphyses of the long bones and larger vertebral bodies. These findings are consistent with our previous observation that increased MEK1 signaling in chondrocytes inhibits endochondral bone growth.[17] While the proximal long bones—the humerus and femur—were significantly longer in ERK1/2/Col2a1Cre embryos, the phenotype was less obvious in the distal bones. Similar overgrowth of the proximal long bones was also described in *Fgfr3*-deficient mice.[14] Therefore, it is interesting to speculate that chondrocytes in the proximal long bones are more sensitive to Fgfr3 and its downstream ERK1/2 signaling compared with chondrocytes in the distal bones. The observed difference may also be relevant to human achondroplasia, which is characterized by rhizomelic dwarfism, a disproportionate dwarfing of the proximal bones.[6] In contrast to our findings with ERK1/2/Col2a1Cre embryos, we did not observe obvious differences in the postnatal growth of long bones in ERK1/2/Col2a1CreER mice. It is possible that our 60% inhibition of *ERK2* in addition to *ERK1* is not sufficient to promote growth in these mice.

The increased bone growth of ERK1/2/Col2a1Cre embryos may be due to the increase in chondrocyte hypertrophy. We have recently found that ERK1/2/Col2a1Cre embryos show a remarkable expansion of the zone of hypertrophic chondrocytes in the long bones, while chondrocyte proliferation is strongly inhibited.[26] It has been shown that chondrocyte hypertrophy is a major determinant of longitudinal bone growth.[28,29] Chondrocyte hypertrophy is also likely to account for the growth in the width in addition to periosteal apposition. Since ERK1/2/Col2a1Cre embryos do not show an obvious periosteal phenotype, periosteal apposition may not be significantly affected in these embryos. The increase in the size of the vertebral body is also associated with the predominant presence of hypertrophic chondrocytes in our current study. Furthermore, these observations are consistent with our previous study showing that increased MEK1 signaling inhibits chondrocyte hypertrophy and bone growth.[17]

Since spinal canal stenosis is a common and serious complication of achondroplasia, the effects of ERK1/2 inactivation on spinal canal development are of particular interest. While ERK1/2/Col2a1Cre embryos showed increased dimensions of the vertebral body in both the anterior−posterior and lateral directions, these embryos also showed a narrower spinal canal at E18.5. The increased growth of the cartilaginous vertebral body toward the spinal canal may account for the narrower spinal canal in ERK1/2/Col2a1Cre embryos. In contrast to ERK1/2 inactivation in the prenatal period, the postnatal inactivation of *ERK1* and *ERK2* resulted in a delay in the closure of the neurocentral synchroses and an increase in the size of the vertebral foramen, indicating that ERK1/2 regulates the timing of synchrosis closure and the size of the spinal canal. We have previously found premature synchrosis closure in mouse models of achondroplasia and in human

samples of homozygous achondroplasia and thanatophoric dysplasia.[20] Our observations in ERK1/2/Col2a1CreER mice indicate that ERK1 and ERK2 would be a promising therapeutic target for spinal canal stenosis caused by activating mutations in FGFR3. Our results in ERK1/2/Col2a1Cre embryos also suggest that ERK1/2 inactivation before the ossification of the vertebral body could result in a narrower spinal canal. The timing of *ERK1* and *ERK2* inactivation would be critical for the successful enlargement of the spinal canal in the future treatment of achondroplasia.

In summary, we have shown that genetic *ERK1* and *ERK2* inactivation in chondrocytes enhances the growth of cartilaginous skeletal elements. We have also shown that the postnatal inactivation of *ERK1* and *ERK2* in chondrocytes delays synchondrosis closure and enlarges the spinal canal. The efficacy of ERK inactivation for the treatment of FGFR3-related skeletal syndromes should be further tested by inactivating ERK1 and ERK2 in mouse models with activating Fgfr3 mutations.

ACKNOWLEDGMENTS

REFERENCES

1. Rousseau F, Bonaventure J, Legeai-Mallet L, et al. 1994. Mutations in the gene encoding fibroblast growth factor receptor-3 in achondroplasia. Nature 371:252–254.
2. Shiang R, Thompson LM, Zhu YZ, et al. 1994. Mutations in the transmembrane domain of FGFR3 cause the most common genetic form of dwarfism, achondroplasia. Cell 78:335–342.
3. Rousseau F, Saugier P, Le Merrer M, et al. 1995. Stop codon FGFR3 mutations in thanatophoric dwarfism type 1. Nat Genet 10:11–12.
4. Bellus GA, McIntosh I, Smith EA, et al. 1995. A recurrent mutation in the tyrosine kinase domain of fibroblast growth factor receptor 3 causes hypochondroplasia. Nat Genet 10:357–359.
5. Wilcox WR, Tavormina PL, Krakow D, et al. 1998. Molecular, radiologic, and histopathologic correlations in thanatophoric dysplasia. Am J Med Genet 78:274–281.
6. Horton WA, Hall JG, Hecht JT. 2007. Achondroplasia. Lancet 370:162–172.
7. Pandit B, Sarkozy A, Pennacchio LA, et al. 2007. Gain-of-function RAF1 mutations cause Noonan and LEOPARD syndromes with hypertrophic cardiomyopathy. Nat Genet 39:1007–1012.
8. Aoki Y, Niihori T, Kawame H, et al. 2005. Germline mutations in HRAS proto-oncogene cause Costello syndrome. Nat Genet 37:1038–1040.
9. Rodriguez-Viciana P, Tetsu O, Tidyman WE, et al. 2006. Germline mutations in genes within the MAPK pathway cause cardio-facio-cutaneous syndrome. Science 311:1287–1290.
10. Naski MC, Colvin JS, Coffin JD, Ornitz DM. 1998. Repression of hedgehog signaling and BMP4 expression in growth plate cartilage by fibroblast growth factor receptor 3. Development 25:4977–4988.
11. Wang Y, Spatz MK, Kannan K, et al. 1999. A mouse model for achondroplasia produced by targeting fibroblast growth factor receptor 3. Proc Natl Acad Sci USA 96:4455–4460.
12. Segev O, Chumakov I, Nevo Z, et al. 2000. Restrained chondrocyte proliferation and maturation with abnormal growth plate vascularization and ossification in human FGFR-3 (G380R) transgenic mice. Hum Mol Genet 9:249–258.
13. Iwata T, Chen L, Li C, et al. 2000. A neonatal lethal mutation in FGFR3 uncouples proliferation and differentiation of growth plate chondrocytes in embryos. Hum Mol Genet 9:1603–1613.
14. Colvin JS, Bohne BA, Harding GW, et al. 1996. Skeletal overgrowth and deafness in mice lacking fibroblast growth factor receptor 3. Nat Genet 12:390–397.
15. Deng C, Wynshaw-Boris A, Zhou F, et al. 1996. Fibroblast growth factor receptor 3 is a negative regulator of bone growth. Cell 84:911–921.
16. Toydemir RM, Brassington AE, Bayrak-Toydemir P, et al. 2006. A novel mutation in FGFR3 causes camptodactyly, tall stature, and hearing loss (CATSHL) syndrome. Am J Hum Genet 79:935–941.
17. Murakami S, Balmes G, McKinney S, et al. 2004. Constitutive activation of MEK1 in chondrocytes causes Stat1-independent achondroplasia-like dwarfism and rescues the Fgfr3-deficient mouse phenotype. Genes Dev 18:290–305.
18. Yasoda A, Komatsu Y, Chusho H, et al. 2004. Overexpression of CNP in chondrocytes rescues achondroplasia through a MAPK-dependent pathway. Nat Med 10:80–86.
19. Chrisman TD, Garbers DL. 1999. Reciprocal antagonism coordinates C-type natriuretic peptide and mitogen-signaling pathways in fibroblasts. J Biol Chem 274:4293–4299.
20. Matsushita T, Wilcox WR, Chan YY, et al. 2009. FGFR3 promotes synchondrosis closure and fusion of ossification centers through the MAPK pathway. Hum Mol Genet 18:227–240.
21. Hecht JT, Francomano CA, Horton WA, Annegers FJ. 1987. Mortality in achondroplasia. Am J Hum Genet 41:454–464.
22. Pauli RM, Scott CI, Wassman ER, et al. 1984. Apnea and sudden unexpected death in infants with achondroplasia. J Pediatr 104:342–348.
23. Selcher JC, Nekrasova T, Paylor R, et al. 2001. Mice lacking the ERK1 isoform of MAP kinase are unimpaired in emotional learning. Learn Mem 8:11–19.
24. Samuels IS, Karlo JC, Faruzzi AN, et al. 2008. Deletion of ERK2 mitogen-activated protein kinase identifies its key roles in cortical neurogenesis and cognitive function. J Neurosci 28:6983–6995.
25. Ovchinnikov DA, Deng JM, Ogunrinu G, Behringher RR. 2000. Col2a1-directed expression of Cre recombinase in differentiating chondrocytes in transgenic mice. Genesis 26:145–146.
26. Matsushita T, Chan YY, Kawanami A, et al. 2009. Extra-cellular signal-regulated kinase 1 (ERK1) and ERK2 play essential roles in osteoblast differentiation and in supporting osteoclastogenesis. Mol Cell Biol 29:5843–5857.
27. Nakamura E, Nguyen MT, Mackem S. 2006. Kinetics of tamoxifen-regulated Cre activity in mice using a cartilage-specific CreER(T) to assay temporal activity windows along the proximodistal limb skeleton. Dev Dyn 235:2603–2612.
28. Breur GJ, VanEnkevort BA, Farnum CE, et al. 1991. Linear relationship between the volume of hypertrophic chondrocytes and rate of longitudinal bone growth in growth plates. J Orthop Res 9:348–359.
29. Wilsman NJ, Farnum CE, Leiferman EM, et al. 1996. Differential growth by growth plates as a function of multiple parameters of chondrocytic kinetics. J Orthop Res 14:927–936.